Available online at www.sciencedirect.com
SCIENCE DIRECT®
Journal of the European Ceramic Society 25 (2005) 1805–1812
www.elsevier.com/locate/jeurceramsoc

# Hydrothermal corrosion of zirconia-toughened alumina (ZTA) at 200 °C

Mathias Herrmann[a,*], Björn Seipel[b], Jochen Schilm[a], Klaus G. Nickel[c], Grit Michael[a], Andreas Krell[a]

[a] *Fraunhofer Institute of Ceramic Technologies and Sintered Materials (IKTS), Winterbergstrasse 28, 01277 Dresden, Germany*
[b] *Portland State University, Department of Physics, Portland, USA*
[c] *Eberhard-Karls-University, Institute for Geosciences, Applied Mineralogy, Tuebingen, Germany*

Available online 22 January 2005

**Abstract**

To investigate the corrosion behaviour of zirconia-toughened alumina (ZTA) under hydrothermal corrosion, a commercial material was compared with materials of similar composition, but fabricated using different processing methods and pure alumina. The specimens were corroded at a temperature of 200 °C in deionised water. Generally, linear corrosion kinetics were found. Pure alumina shows the lowest mass loss and the smallest rate constants. The reduction of the four-point bending strength does not correlate with the mass loss. The main parameter for the degradation is the cubic/tetragonal to monoclinic transformation of zirconia. Investigation of the corrosion of polished surfaces reveals spallation of $Al_2O_3$ grains or groups of grains surrounded by zirconia as the main mechanism. A decrease in the size of zirconia grains helps to reduce the strength degradation.


*Keywords:* Corrosion; Mechanical properties; $ZrO_2$; $Al_2O_3$; Defects

## 1. Introduction

Ceramics are believed to generally show excellent corrosion resistance. In reality the corrosion resistance against acids, basics and molten salts is variable. As a result, it is necessary to test a given material for applications that bring it into contact with corrosive media.

Alumina and zirconia ceramics have widespread applications. Alumina ceramics have excellent hardness, corrosion resistance and wear properties, but lower strength and toughness than zirconia or zirconia-toughened alumina (ZTA).[1] The corrosion resistance of alumina under hydrothermal conditions decreases with increasing impurity content of the ceramics and is controlled by the dissolution of the amorphous grain boundary phases, which is often dominated by $SiO_2$ and $Na_2O$.[1,2]

Tetragonal zirconia ceramics (TZP) show a much higher toughness and bending strength but are known for their low stability under corrosive conditions. This general statement is based on investigations of the corrosion behaviour of $Al_2O_3$ and Y-TZP (yttria-stabilised-tetragonal-zirconia-polycrystals) in NaOH and acids at 150–300 °C.[2–4] The hydrothermal ageing of Y-TZP ceramics is connected with internal stresses due to the cubic/tetragonal to monoclinic (c/t → m) phase transformation of zirconia.[5–7]

The addition of zirconia to alumina ceramics (ZTA) increases the toughness and the bending strength. The resulting ZTA ceramics play an important role for applications in the chemical industry such as pump components, but only little information exists about the corrosion resistance under varying conditions. Thompson and Rawlings[8] reported a good corrosion resistance of ZTA against distilled water/ethylene glycol solutions at 20 and 80 °C. Hollstein and coworkers[9] investigated the corrosion of ZTA in phosphoric and sulphuric acid, NaOH, and distilled water in a temperature range between RT and 90 °C. The ZTA ceramic showed a good resistance against these media with a maximum mass loss of 0.2 mg/cm$^2$ and a decrease in bending strength of approximately 10% in the case of phosphoric acid exposure at 90 °C for 900 h.

* Corresponding author. Tel.: +49 351 2553 527.
*E-mail address:* mathias.herrmann@ikts.fhg.de (M. Herrmann).

0955-2219/$ – see front matter © 2004 Published by Elsevier Ltd.
doi:10.1016/j.jeurceramsoc.2004.12.009

$ZrO_2/Al_2O_3$/TiC composite ceramics were reported to have a high stability under hydrothermal conditions, independent of the partial phase transformations of the $ZrO_2$ occurring during the corrosion process.[10,11]

The aim of this work is to investigate the corrosion of ZTA materials in water under hydrothermal conditions and its influence on basic characteristics like the bending strength. Different shaping approaches were applied to obtain different grain sizes and defect populations for investigation of their influence on hydrothermal ageing.

## 2. Experimental setup and starting materials

The samples used were three ZTA materials with nearly identical composition ($Al_2O_3$ + 10 wt.% $ZrO_2$ stabilised by 5 mol% $Y_2O_3$) and one $Al_2O_3$ ceramic (A2) based on A16SG powder (Table 1). According to the data sheet of the manufacturer the A16SG $Al_2O_3$ powder has less than 0.03% $SiO_2$ and less than 0.1% alkaline and earth alkaline impurities. The zirconia powder has an even higher purity. Milling and mixing of the starting composition was done in high purity alumina bowls to avoid an increase of the initial impurity level.

ZTA1 was a commercial material (Friatec, FZT), the other materials were produced at the Fraunhofer Institute of Ceramic Technologies and Sintered Materials (IKTS) in Dresden, Germany.

ZTA2 was manufactured by mixing the powders in water in a planetary ball mill (1 h), freeze drying, dry-pressing at 100 MPa into plates 60 mm × 60 mm × 6 mm and sintering at 1670 °C for 2 h.

The materials ZTA3 and A2 were prepared by gel casting.[12] Owing to the gel casting process, the sintering temperature could be decreased to 1580 °C.

The microstructures of the ZTA materials (example shown in Fig. 1) were investigated on polished cross sections by field emission SEM (FESEM DSM982 Gemini). The D(50) grain size was measured from the statistics of the linear intercepts of the grains (Table 1). The specimen for corrosion experiments had the shape of rectangular bars (3.5 mm × 3.5 mm × 50 mm). The surface was ground, only some samples were polished for detailed investigations of the surface damage during the corrosion.

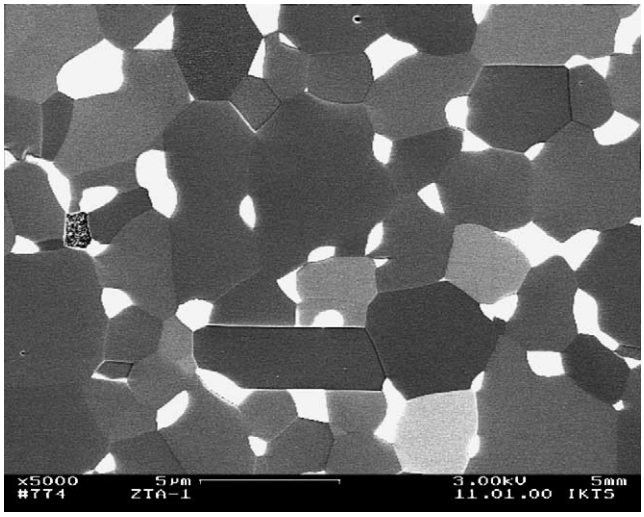


Fig. 1. FESEM picture of a polished ZTA1 surface (grey: $Al_2O_3$; white: zirconia).

Four-point bending tests (40/20 mm, cross head velocity 0.5 mm/min) showed that the pure alumina A2 exhibits the lowest mean strength with 395 MPa (ZTA2 > ZTA3 > ZTA1 > A2, Table 1). The differences in strength of ZTA2, ZTA3 and ZTA1 are attributed to differences in grain size of the $ZrO_2$ particles and initial relative monoclinic phase amount (Table 1).

The closed system hydrothermal experiments were carried out in a 500 ml autoclave with a PTFE-inlet (Berghof, Germany) at the equilibrium water vapour pressure ($p \approx 16$ bar at 200 °C). The test temperature was 200 °C with a precision of ±2 °C and the volume of the deionised water was 400 ml. To prevent the development of a diffusion barrier, the sample holder in the autoclave rotated at approximately 300 rpm. The experiments were interrupted for the determination of mass changes after different exposure times, at these points the water was replaced.

Table 1
Characteristics of the investigated materials

| | Material | | | |
|---|---|---|---|---|
| | ZTA1 | ZTA2 | ZTA3 | *A2* |
| Strength ($\sigma_{4b}$) (MPa) | 454 ± 45 | 550 ± 70 | 515 ± 80 | 395 ± 60 |
| Density | 4.10 | 4.109 ± 0.003 | 4.114 ± 0.003 | 3.954 ± 0.003 |
| Phase composition (XRD)[a] (wt.%) | | | | |
| Corundum | 88.2 ± 0.6 | 89.5 ± 0.6 | 90.2 ± 0.6 | 100 |
| c-$ZrO_2$ | 4.1 ± 1.5 | 2.3 ± 1.5 | 2.5 ± 2 | |
| t-$ZrO_2$ | 5.8 ± 1.5 | 8.1 ± 1.5 | 7.0 ± 2 | |
| m-$ZrO_2$ | 1.9 ± 0.4 | 0.1 ± 0.2 | 0.2 ± 0.2 | |
| $Al_2O_3$ grain size D(50) (μm) | 2.04 | 1.49 | 0.9 | 3.2/15 (bimodal) |
| $ZrO_2$ grain size D(50) (μm) | 0.84 | 0.48 | 0.25 | |

[a] Error is 3$\sigma$.

The open system hydrothermal experiments were done in an autoclave with continuous flow of water and have been described elsewhere.[13]

Before the corrosive treatment all samples were prepared by a standard procedure: The samples were washed in acetone for 10 min, rinsed with deionised water for 2 min, dried for at least 2 h at 150 °C, and weighed on a microbalance after a 2 h cooling period. After the experiment the samples were again rinsed with deionised water, dried, and weighed using the same procedures. The corrosive attack was monitored by mass change and four-point bending strength after exposure. The surface of the corroded specimens was characterised by scanning electron microscopy (SEM). X-ray diffraction analysis (Seifert-FPM; XRD7; Cu Kα radiation; $2\Theta$ range: 12–90°; step size 0.02°; counting time per step 10 s) was conducted for the determination of the monoclinic $ZrO_2$ phase content, which was calculated by Rietveld refinements (Autoquant, Seifert-FPM).

## 3. Results

### 3.1. Mass change and bending strength

After hydrothermal treatments we always observed a mass loss. Fig. 2a shows the mass changes of the tested ceramics after exposure in deionised water at 200 °C for up to 200 h. All mass loss curves are linear with time.

The individual lines in Fig. 2 have varying intersects with the *y*-axis at $t = 0$. This is attributed to surface effects. Machining induced surface films or statistically rare secondary phases, which are easily solvable, could be responsible. It should be noted that the off-set in Fig. 2 is in the range of only 50 μg.

The slope of the lines in Fig. 2 is thus a much better indicator for the corrosion velocity than the absolute value. Linear rate constants of the corrosion reactions determined by linear regression are given in Table 2 and Fig. 2c. The highest rate constant was found for the commercial ZTA1 and is more than two times higher than those of the other materials. The smallest corrosion rate constant was found for the pure alumina (A2).

The rate constants for ZTA1 and ZTA2 are in good agreement with data from the open system (Fig. 2b and c). The open system experiments yielded slightly higher rate constants but confirm the overall ranking. This is seen as evidence that saturation effects during the exposure of the specimens in the closed system autoclave did not significantly influence the corrosion process.

The bending strength of the materials was determined after 5 h and after the end of the corrosion experiments (Table 2). The alumina reference material was the only material with constant strength under these hydrothermal conditions. ZTA1 experienced a higher mass loss than ZTA2 but showed nearly the same decrease in strength. ZTA3 had a higher mass loss than ZTA2, but it decreased in strength by about 10% only.

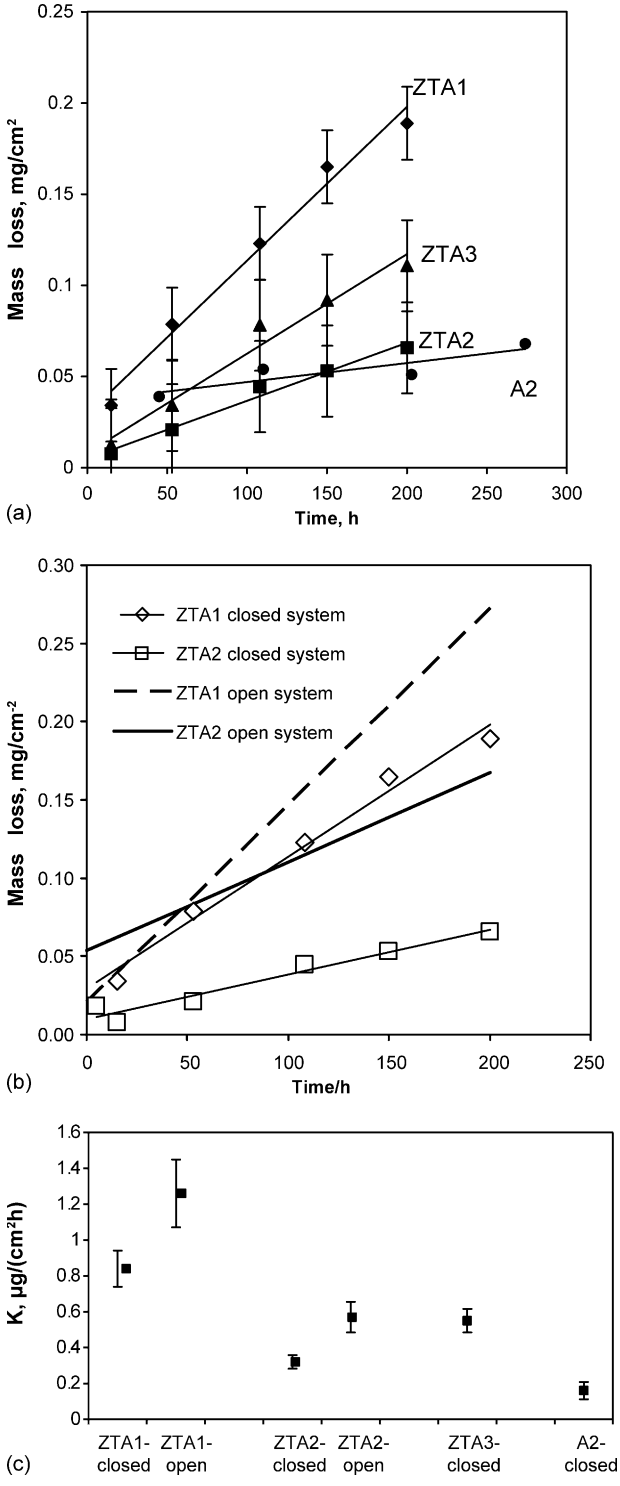


Fig. 2. (a) Mass loss with time of the ceramics corroded in deionised water at 200 °C in closed system autoclave. (b) Comparison between the mass loss of ZTA1 and ZTA2 with time and data from investigation in an open system[13] (flow rate 200 ml/h). (c) Comparison of mass loss rates in open[13] and closed system.

Table 2
Four-point bending strength of the corroded materials after maximal exposure time in comparison with data from the uncorroded ceramics

| Material | $\sigma_{4b(residual)}$ after 5 h (MPa) | $\sigma_{4b(residual)}/\sigma_{4b}$ (%) (5 h) | $\sigma_{4b(residual)}$ after 200 h (MPa) | $\sigma_{4b(residual)}/\sigma_{4b}$ (%) (200 h) | $K$ (μg/(cm$^2$ h)) | Standard deviation |
|---|---|---|---|---|---|---|
| ZTA1 | | | 355 ± 50 | 78 | 0.84 | 0.06 |
| ZTA2 | 480 ± 60 | 90 | 420 ± 60 | 76 | 0.32 | 0.02 |
| ZTA3 | 530 ± 120 | 100 | 460 ± 40 | 89 | 0.55 | 0.05 |
| A2 | 390 ± 40 | 99 | 410 ± 60[a] | 100 | 0.18 | 0.006 |

[a] 270 h.

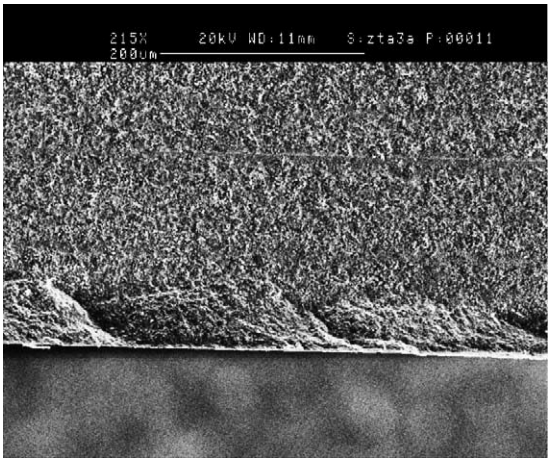


Fig. 3. SEM micrograph showing edge flaking of corroded bending bar in ZTA3.

This shows that the mass loss cannot be correlated directly with the change in bending strength.

The analysis of the fracture surfaces of the corroded samples showed that the fracture origins are mostly located at the edges of the samples. In contrast to the pristine samples, edge flaking was often observed in corroded bending bars (Fig. 3).

### 3.2. X-ray diffraction analysis

The main phase of the ZTA ceramics – corundum – was used as a standard for the refinement of the cubic/tetragonal zirconia lattice constants via the Rietveld method.[14] A comparison of the lattice constants of those zirconia polymorphs with data from the Inorganic Crystal Structure Database (ICSD, $Zr_{1-x}Y_xO_{2-y}$) confirmed the expected incorporation of yttria in the lattice of the $ZrO_2$ phases in the ZTA ceramics. The refined amounts of monoclinic, tetragonal and cubic zirconia are given in Table 3. Generally, ZTA1 showed the highest, well detectable, amount of monoclinic zirconia. In contrast, the monoclinic phase content for ZTA2 and ZTA3 was detectable, but smaller than the error in our Rietveld refinements. The monoclinic phase content increases during the corrosive attack in the order ZTA3, ZTA2 to ZTA1. This can be correlated with the lower $ZrO_2$ grain size of the materials ZTA2 and ZTA3 in comparison to ZTA1.

### 3.3. Surfaces of the corroded samples

Both the surfaces from originally ground and polished samples were examined with FESEM after the hydrothermal treatment. The polished samples were used to characterise the early stage (up to 25 h) of exposure, while the rougher surfaces of the ground samples were used for the long-term experiments (200 h).

Fig. 5 shows the surface of ZTA1 corroded for 5 and 25 h. Spalling of $Al_2O_3$ grains surrounded by $ZrO_2$ grains was observed, probably as a result of the c/t → m transformation. The shift of the well visible polishing scratches verifies that the grains have moved from their original locations. These scratches did, however, not appear in the as polished state (cp. Fig. 1). This is clear evidence that the $Al_2O_3$ grains did corrode more intensively at these sites due to the preceding microplastic deformation. Similar effects were found in ZTA2 material.

All defects are surrounded by $ZrO_2$ grains. With increasing corrosion time these local defects increase. Some large cracks are interpreted to have formed this way (Fig. 4d). The behaviour of all ZTA materials is similar and also ground samples basically showed the same features as the polished ones.

Only ZTA1 material showed in addition isolated porous areas free of zirconia (Fig. 5a). Probably these porous areas

Table 3
Monoclinic phase content and ratio of the m-$ZrO_2$ to total $ZrO_2$ content of ZTA1–3 before and after 200 h corrosion in deionised water

| Material | Phase content of monoclinic zirconia before corrosion (wt.%) | m/(m + t + c) (%) | Phase content of monoclinic zirconia after 200 h exposure time (wt.%) | m/(m + t + c) (%) |
|---|---|---|---|---|
| ZTA1 | 1.9 ± 0.4 | 17 | 3.3 ± 0.4 | 28.7 |
| ZTA2 | 0.1 ± 0.2 | 1 | 0.3 ± 0.2 | 2.9 |
| ZTA3 | 0.2 ± 0.2 | 2 | 0.4 ± 0.2 | 3.9 |

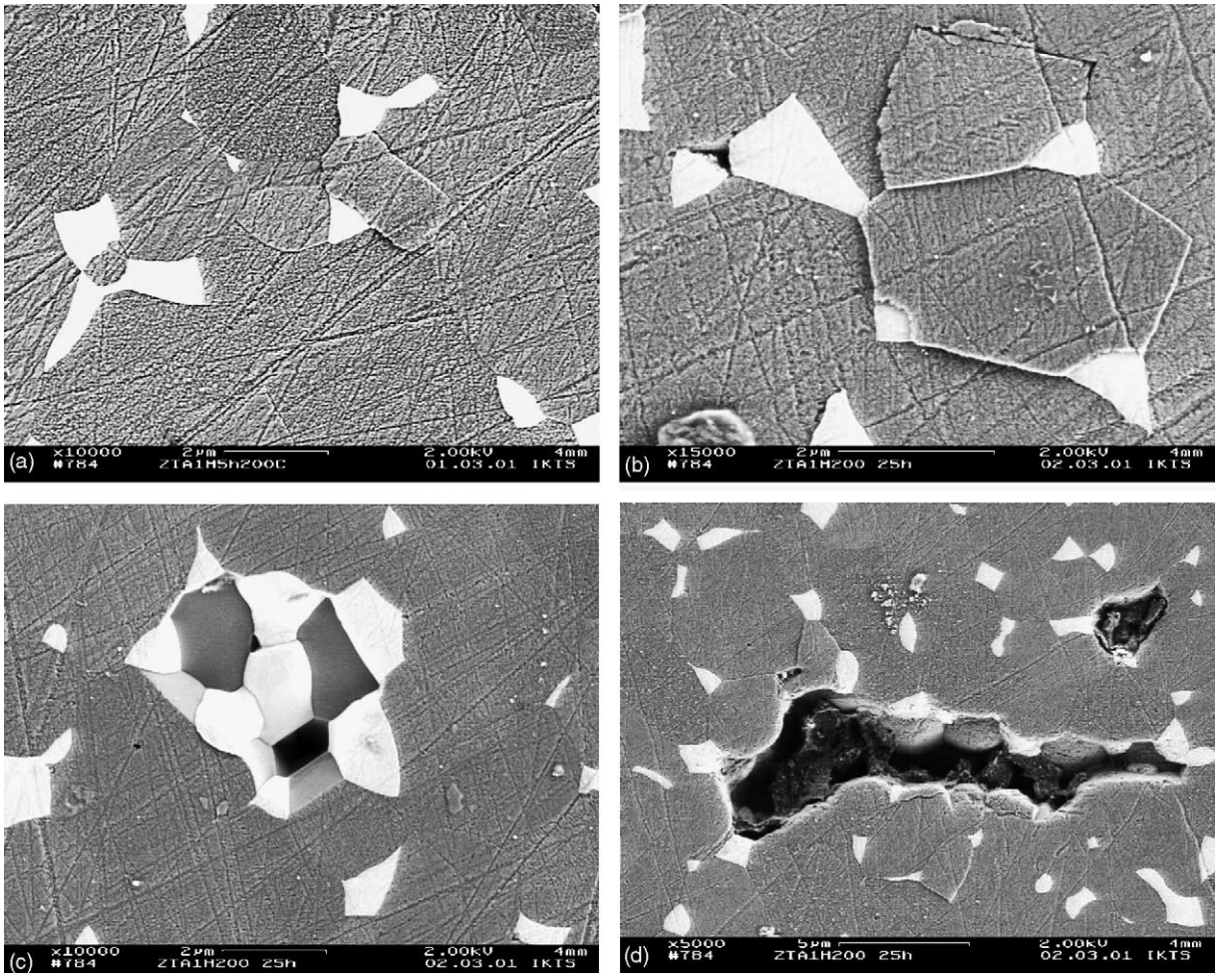


Fig. 4. FESEM micrographs of polished ZTA1 after 5 h (a) and 25 h (b–d) hydrothermal corrosion at 200 °C.

were caused by the corrosive attack on localised impurities. In the pure alumina ceramic, only some minor corrosive attack was visible. Only in a few cases spallation of grains could be observed and then they seems to be related to the removal of a local thick impure grain boundary phase (Fig. 5b).

## 4. Discussion

Pure alumina ceramics show a good resistance to hydrothermal corrosion in deionised water at 200 °C. The linear behaviour of the mass loss curve of the alumina material (A2) is in good agreement with reported data from other authors.[1] The comparatively high mass loss found for small exposure times ($t \approx 0$) indicates a fast solution of a surface layer damaged by grinding and polishing and also of minor impurities. The constant bending strength indicates that this material shows low corrosion effects at these conditions.

The observation that the pure alumina ceramic A2 with its low mass losses was the one ceramic without strength degradation is a clear evidence that both the higher mass loss (Fig. 2) and the strength degradation of the ZTA ceramics (Table 2) are caused by corrosion effects that are associated with the $ZrO_2$ phase. Thus a comparison between the various ZTA grades has to answer questions about the role of impurities, grain size and transformation behaviour in the corrosion performance of these materials.

The investigated ZTA showed a linear time dependence of the mass loss with time, however with a higher slope than the pure alumina ceramic. The commercial material ZTA1 showed the highest mass loss at the beginning of the corrosion which is attributed to its higher impurity content. EDX and Raman investigations showed β-alumina as a minor phase in the ZTA1 microstructure,[13] while it is absent in ZTA2 and ZTA3. This and other impurity containing phases are, as a rule, less stable than alumina and zirconia.

The absolute mass losses and loss rates of Fig. 2 are not directly correlated with the degradation of bending strength of the materials as recorded in Table 2. Nonetheless the major parameter for the corrosion under these conditions has to

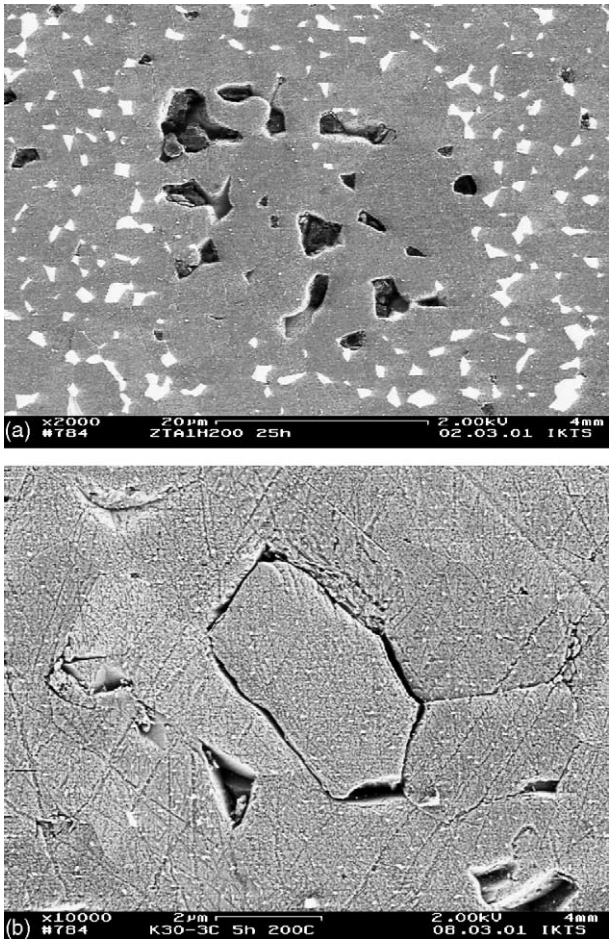


Fig. 5. FESEM micrographs of some local defects found after corrosion in ZTA1 (a) and alumina A2 (b).

be the corrosion induced c/t → m phase transformation of zirconia.

ZTA3 showed no strength degradation during 200 h hydrothermal corrosion at 300 °C.[15] Therefore, the strength degradation of the ZTA materials during corrosion at 300 °C is less pronounced than at 200 °C. We attribute this to the observed higher stability of tetragonal Y-$ZrO_2$ in humid atmospheres at 300 °C in comparison to 200 °C[5] and view it as an additional evidence for the decisive role of the $ZrO_2$ particles in the corrosion process.

Our interpretation of the corrosion process is schematically drawn in Fig. 6. In a bulk ZTA material the nominal 3–5% increase in the volume of the $ZrO_2$ results in local compressive and tensile stresses. This is akin to the ordinary transformation toughening process, which is wanted. In a surface situation (Fig. 6b) there is no matrix to support the internal stresses in *z*-direction. Hence here we have true expansion. If this expansion is hindered by overlapping matrix grains, this will exert a lifting stress on the latter.

Whether or not an actual lifting with or without spallation takes place depends now on the local situation: the size of the transformed grain, the number of transforming grains in the vicinity, and the relative position of grain boundaries will all contribute to this.

Therefore, the overall situation is such that in the pristine samples the transformation contributes to higher strength of the ZTA ceramics compared with the alumina ceramic A2. During corrosion some additional surfacial $ZrO_2$ particles transform, giving rise to the residual stresses in the alumina matrix with partial lifting and spallation. Some of the formed defects grow by further corrosive attack on the new formed surface and form larger cracks (Fig. 4d), influencing the residual strength values. The defect size depends on the size of both transformed and spalled grains and the ability of defects to interlink. This in turn is linked to the number and distribution of transforming grains.

This is the reason for the tendency of ZTA3 to be less affected: It has smaller $ZrO_2$ particle size and this makes it harder to transform them and if it happens, it induces smaller defects.

The mechanism of the corrosion induced c/t → m transformation in $ZrO_2$ has different aspects. On the one hand it was shown[5] for Y-TZP ceramics and powder that the incorporation of water into t-$ZrO_2$ destabilises the tetragonal structure and accelerates the phase transformation resulting in changed internal stress and micro cracks. On the other hand the local tensile stresses at the grain boundaries of $Al_2O_3$ grains caused by neighbouring t-$ZrO_2$ particles (Fig. 6) can accelerate the corrosion attack at these boundaries. The consequence is the cracking of the boundaries and a reduction of the compressive stresses on the transformable t-$ZrO_2$ grains. These reduced compressive stresses result in a spontaneous transformation to m-$ZrO_2$ and as a consequence, in additional stresses in the alumina matrix causing the crack growth in the matrix and spalling of $Al_2O_3$ grains. There is no possibility to distinguish between the two mechanisms. It can be assumed that both contribute to the strength degradation.

In pure alumina ceramics an increased attack of the grain boundary at the surface takes place as well, especially in grain boundaries with a segregated glassy phase (Fig. 5b). The lower internal stresses in alumina ceramics in comparison to ZTA ceramics result in reduced damage. The existing initial flaws in the ceramics are still the strength limiting defects.

The results indicate that the residual stresses may be favourable for the toughening but have a negative influence on the corrosion stability. In other words, the corrosion damage can only be minimised if the matrix is very strong and corrosion resistant and if fracture of the grain boundaries with subsequent pull out of the grains does not occur. Such behaviour was previously observed in submicro $ZrO_2/Al_2O_3$/TiC composite ceramics.[10,11] Generally it is known that the stability of the t-$ZrO_2$ increases with decreasing grain size. Therefore, the $ZrO_2$ materials with the lowest particle size are expected to exhibit the least severe ageing. The ranking of the decreasing strength degradation

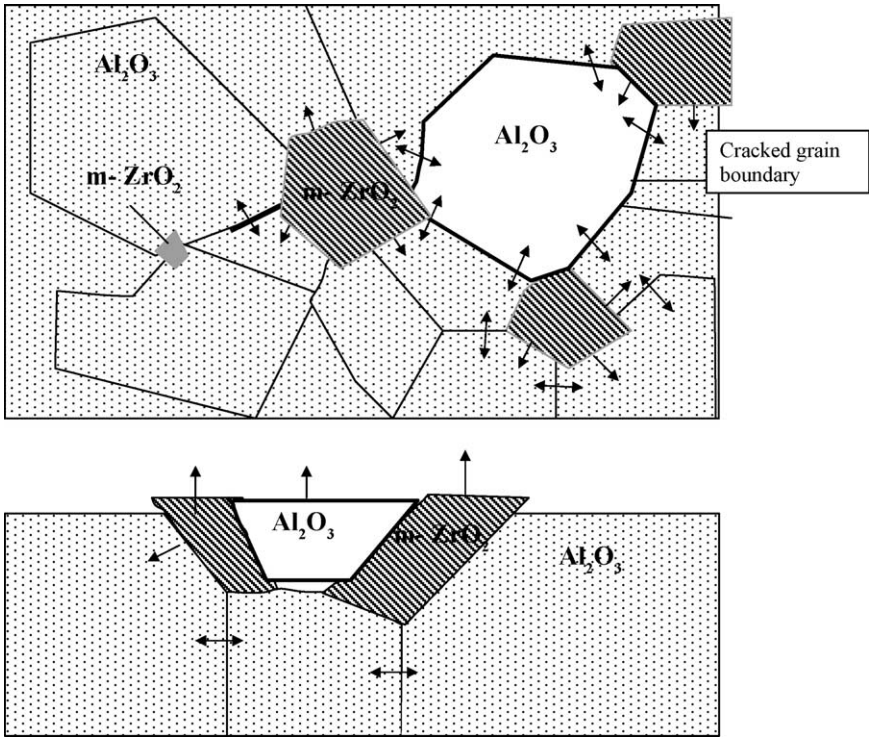


Fig. 6. Schematic presentation of the formation of internal stresses and crack formation due to the corrosion induced phase transformation of larger t-$ZrO_2$ particles (a: view on the surface; b: cross section). (→) Compressive stress; (↔) tensile stress leading to cracks in the grain boundary phase (—).

from ZTA1 through ZTA3 (Tables 2 and 3) confirms these considerations.

## 5. Conclusion

1. Under hydrothermal conditions at 200 °C, a degradation of ZTA materials takes place leading to a reduction of the residual strength.
2. The mass loss during corrosion depends linearly on time. The reduction in strength does not correlate directly with the mass loss rate.
3. The investigations of polished surfaces after corrosion showed that the main reason for the degradation of the materials is the cubic/tetragonal to monoclinic phase transformation. This transformation causes additional surface stresses, which results in the spalling of individual $Al_2O_3$ grains or groups of grains. The defects formed by this process can grow by interlinking and become strength determining.
4. The material with the smallest $ZrO_2$ grain size showed the least strength degradation.

## Acknowledgements

The authors gratefully acknowledge funding by the German Research Society (DFG) in a joint project (Ni 299/7, He2457/4).

## References

1. Oda, K. and Yoshio, T., Hydrothermal corrosion of alumina ceramics. *J. Am. Ceram. Soc.*, 1997, **80**(12), 3233–3256.
2. Genthe, W. and Hausner, H., Corrosion of aluminium oxide in acids and caustic solutions. *cfi/Ber. DKG*, 1990, **67**(1/2), 6–10.
3. Sato, T., Sato, S., Okuwaki, A. and Tanaka, S., Corrosion behaviour of alumina ceramics in caustic alkaline solutions at high temperatures. *J. Am. Ceram. Soc.*, 1991, **74**(12), 3081–3084.
4. Sato, T., Sato, S. and Okuwaki, A., The corrosion behaviour of ceramic materials in caustic alkaline solutions at high temperature. *Corrosion Sci.*, 1992, **33**(4), 591–603.
5. Lawson, S., Environmental degradation of zirconia ceramics. *J. Eur. Ceram. Soc.*, 1995, **15**(6), 485–502.
6. Schacht, M., Boukis, N., Dinjus, E., Ebert, K., Janssen, R., Meschke, F. *et al.*, Corrosion of zirconia ceramics in acidic solutions at high pressures and temperatures. *J. Eur. Ceram. Soc.*, 1998, **18**, 2373–2376.
7. Watanabe, M., Iio, S. and Fukuura, J., Aging behaviour of Y-TZP. *Adv. Ceram.*, 1984, **12**, 391–398.
8. Thompson, I. and Rawlings, R. D., Effects of liquid environments on zirconia-toughened alumina. Part II: mechanical properties. *J. Mater. Sci.*, 1992, **27**, 2831–2839.
9. Graas, T., Hollstein, T., Pfeifer, W. and Reckziegel, A., Examining the corrosion behaviour of $Al_2O_3$ + 10% $ZrO_2$ in aqueous solutions. *cfi/Ber. DKG*, 1997, **74**, 723–726.
10. Herrmann, M., Krell, A., Adler, J., Wötting, G., Hollstein, T., Pfeifer, W. *et al.*, Keramische Wälzlager für Anwendungen in korrosiven Medien. *VDI-Ber.*, 1997, **1331**, 251–258.
11. Krell, A. and Blank, P., *Hartstoffverstärkte stabilisierte $ZrO_2$Keramik mit mechanischer Stabilität unter hydrothermaler Beanspruchung*. Patent DE 19733700, 1999.

12. Krell, A., Blank, P., Ma, H.-W., Hutzler, T. and Nebelung, M., Processing of high-density submicrometer $Al_2O_3$ for new applications. *J. Am. Ceram. Soc.*, 2003, **86**(4), 546–553.
13. Seipel, B., *Korrosion von Siliciumnitrid und Zirkonoxidverstärktem Aluminiumoxid in wässriger Lösung unter Durchflussbedingungen*. Dissertation thesis, University Tuebingen, 2003.
14. Young, R. A. ed., *The Rietveld Method, Monographs on Crystallography, Vol 5*. Oxford Press, 1993.
15. Herrmann, M., Schilm, J. and Michael, G., Corrosion behaviour of different technical ceramics in acids, basic solutions and under hydrothermal conditions. *Key Eng. Mater.*, 2004, **264–268**, 877–880.